CHAPTER 8

Effect of hockey stick-shaped molecules on the critical behavior at the nematic to isotropic and smectic-*A* to nematic phase transitions in octylcyanobiphenyl

8.1. Introduction

In recent years, liquid crystalline mixtures incorporating rod-like and other reduced symmetry molecules have gained considerable attention owing to their competence in bringing out the effect of the molecular conformation on the intermolecular interaction and thereby on the phase behavior of combined systems. Mixtures obtained by combining rod-like and bent-core mesogenic molecules have frequently been endowed with a number of remarkable properties such as enhancement of chirality in cholesteric [1, 2] and smectic C^* fluids [3], induction of novel smectic mesophases [4], generation of antiferroelectric order in smectics [5, 6], inimitable temperature dependence of elastic constant [7], or nanophase segregations [8, 9]. It has been observed that introduction of a very little quantity of bent-core dopant in a rod-like environment can also significantly revise the phase behavior of the host mesogen, including the order of their mesophase transitions [10, 11] and extent of a mesophase region, and may even induce odd characteristic phenomena in known calamitic mesophases. Thus the exact treatment of phase transitions in such doped systems is of unparallel advantage for obtaining a deeper insight

into the unresolved issues regarding transitional phenomena in soft condensed matter systems.

Furthermore, over the past few decades the characteristic behavior of the smectic-*A*–nematic (Sm-*A*–*N*) phase transition has been a subject of extensive theoretical and experimental studies in an effort to determine the order of that transition and the universality class to which it belongs. Considerable progress has been made so far, but still remains a controversial issue in the field of equilibrium statistical mechanics of soft condensed matter [12–16]. The one-dimensional positional order in the Sm-*A* phase can be well described in terms of a two-component complex order parameter (Ψ) and one may expect a three-dimensional *XY* (3D-*XY*) nature of the transition. But owing to the coupling between the molecular ordering and their fluctuations, consistent non-universal type behavior has often been observed for the critical coefficients [17]. Previous mean-field predictions of Kobayashi [18] and McMillan [19] suggested that depending on the ratio of the smectic-*A*–nematic (Sm-*A*–*N*) to nematic–isotropic (*N*–*I*) transition temperatures (i.e., on the extent of the nematic range), the Sm-*A*–*N* transition can either be of first order or second order along with the existence of a tricritical point (TCP) where the transition makes a crossover from second-order to first-order nature. A more realistic model of de Gennes along with the introduction of a Landau-Ginzburg–like functional for type I superconductor, and hence considering a coupling between the nematic (S) and smectic (Ψ) order parameters, envisages the transition to be in the three-dimensional *XY* (3D-*XY*) universality class (corresponding critical exponent α_{XY} = -0.007) like that for the normal-superconducting transition in metal or the lambda transition in He^4 [14]. However, the transition is driven to a crossover from *XY*-like second order to Gaussian tricritical ($\alpha_{TCP} = 0.5$) with a decrease in the nematic width indicating a stronger coupling between S and Ψ; i.e., the 3D-*XY* model is an approximation only unless the nematic order has completely been saturated [13, 17, 20]. The subsequent work of Halperin, Lubensky, and Ma (HLM) [21] revealed that the coupling between the nematic

director fluctuation and the smectic order parameter also put forward a significant contribution by introducing a correction in the free energy term $\sim\Psi^3$, thereby making the transition always weakly first order. It was anticipated that the transitional discontinuity reduces with a decrease in the McMillan ratio (defined as T_{SN}/T_{NI}, where T_{SN} and T_{NI} are the Sm-*A*–*N* and *N*–*I* phase transition temperatures, respectively); however, it never completely dies out. Afterward, a model embracing type II superconductor–like continuous behavior has also been proposed, expecting a 3D-*XY*–like behavior with inverted heat capacity amplitude ratios and ruling out the possibility of any first-order-type behavior [22, 23]. But, the experimentally measured specific heat capacity values consistently reveal a noninverted *XY*-like nature, thereby indicating the insufficiency of the above said model [24–27]. Further attempts have also been made from the study of the anisotropy in the critical behavior associated with the parallel and perpendicular components (with respect to the director) of the correlation length and its subsequent analysis employing various physical models such as gauge transformation theory [28–30], dislocation-loop melting theory [31, 32], and self-consistent one-loop theory [33, 34].

However, none of the above theoretical models fit completely with all the available experimental data and hence they fail to portray a clear scenario of universality. It has been observed that the effective critical exponent is extremely sensitive to the nematic temperature range and demonstrates a systematic variation depending on it. A value of 0.87 of the McMillan ratio points toward the tricritical limit, but experimental findings provide somewhat higher values, ranging between 0.942 and 0.994, suggesting a nonuniversal-type behavior, which again is found to rely on the molecular properties [16]. In the past few decades, the specific heat capacity measurements, light scattering, X-ray diffraction, volumetric studies, and dielectric techniques have been widely employed to study the nature of the phase transitions as well as the universality class of the critical exponents in a wide range of calamitic mesogens embracing the diverse form of core structures, and also in their

mixtures. However, reports relating the study of such transitional phenomena in mixtures consisting of rod-like and bent-core molecules are still scanty [10,11] even though such unconventional candidates may prove to be quite helpful in extracting valuable information regarding transitional anomaly and order character of a transition.

Furthermore, in the field of liquid crystal research the *N–I* phase transition has also appeared to be quite attractive due to its several surprising features. In a mean-field approach Landau and de Gennes [14] have given a simple description of the dynamical behavior of the *N–I* phase transition by expressing the free energy density in powers of the nematic order parameter $S(T)$. It has been observed that the mean-field theory [35] can satisfactorily explain the behavior of the mesophase over most of the temperature ranges, but at very close to transition it fails to describe the critical region. In an effort to analyze this critical region and as well as to disclose the unique aspects of the *N–I* phase transition, a number of attempts employing diverse experimental techniques have been considered so far. Yet, none of them have been able to offer a complete description depending upon the molecular features. However, besides a few disagreements, most of them reveal a tricritical nature [36–38] for the *N–I* phase transition which again can be explained in the context of Landau-de Gennes theory with the free energy density expanded up to sixth order in powers of the nematic order parameter $S(T)$.

The work envisaged in this chapter is principally dedicated to focus on an extensive optical investigation of the critical behavior in vicinity of both the *N–I* and Sm-*A–N* phase transitions in a binary system comprising calamitic octylcyanobiphenyl (8CB) and a laterally methyl substituted hockey stick-shaped compound, 4-(3-*n*-decyloxy-2-methyl-phenyliminomethyl)phenyl 4-*n*-dodecyloxycinnamate (compound **5** as mentioned in chapter 4**)**, from a simple yet quite high resolution (in both the birefringence and temperature) temperature scanning measurement of optical birefringence (Δn) [39]. This technique provides a sufficient number of data points for Δn near the phase

transitions, thus enabling the characterization of the transitional anomaly quite precisely. The critical behavior near the *N*-*I* phase transition has been analyzed and compared with the available literature data. By analyzing the temperature derivative of optical birefringence Δn near the Sm-*A*–*N* phase transition, a power-law divergence with the critical exponent α' has also been observed and found to be in accord with that obtained from the specific heat capacity measurements. Moreover, from an analysis of the Δn data below the Sm-*A*–*N* phase transition, the effective order parameter critical exponent β' has been assessed and from the extracted α' and β' values it has also been possible to estimate the susceptibility critical exponent γ'. The effective critical exponents (α', β', γ') have been explored along the path of the variation of dopant concentration and the observed outcomes for the exponents have been discussed in light of crossover behavior. The effect of the bent-shaped dopant on the intermolecular interactions and hence on the resultant molecular ordering in the host medium has also been discussed.

8.2. Materials

The hockey stick-shaped compound **5** is one of the members (*m* = 12, *n* = 10) of the laterally methyl substituted hockey stick-shaped compounds, 4-(3-*n*-alkyloxy-2-methyl-phenyliminomethyl)phenyl 4-*n*-alkyloxycinnamates, as discussed in chapter 4. The compound 8CB was purchased from E. Merck, UK (having purity higher than 99.9%) and was used without further purification.

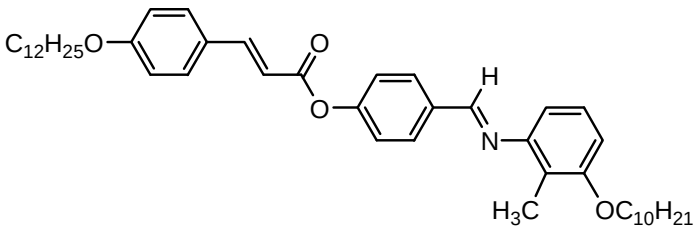

Cr 74.2 °C Sm-C_a 101.4 °C Sm-C_s 109.8 °C N 110.1 °C I

(a)

Figure 8.1. The chemical structure and phase behavior of (a) the hockey stick-shaped compound (compound **5**).

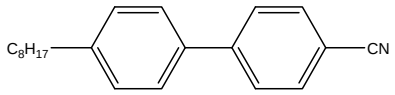

Cr 21.5 °C Sm-A 33.7 °C N 40.5 °C I

(b)

Figure 8.1. (cont'd). The chemical structure and phase behavior of (b) the rod-like compound (8CB).

The structural formulae and the mesophase behavior of both the dopant and host molecules are given in figure 8.1.

Several mixtures have been prepared by adding small amounts of the hockey stick-shaped compound (having molar concentrations ranging between 0.021 and 0.08) into the host medium. The phase diagram has been constructed by studying the sample-texture under a polarizing optical microscope (Motic BA 300) equipped with a Mettler FP900 hot stage.

8.3. Phase diagram

The pure 8CB compound on being cooled from the isotropic phase shows the following stable mesophase sequence *I*–*N*–Sm-*A*–Cr, where the smectic phase is partially bilayer in nature (smectic layers comprising two strongly interdigitated polar sublayers with oppositely faced terminal dipoles). Such a smectic structure is realized owing to some sort of dimerization, induced by the dipole-dipole or dipole-induced dipole interactions, which again tend to cause an antiparallel arrangement of the neighboring polar molecules with one terminal dipole being next to the other or next to a strongly polarizable biphenyl unit [40, 41]. On the other hand the present hockey stick-shaped compound as previously mentioned in chapter 4, comprises a nematic phase, appearing in a quite small temperature range (~ 0.3 K) and two polymorphic tilted smectic phases – the synclinic smectic *C* (Sm-C_s) as well as the anticlinic smectic *C* (Sm-C_a) phases [42]. In the Sm-C_s phase, the direction of the tilt is the same in adjacent smectic layers, whereas it alternates between the layers of the Sm-C_a phase. Figure 8.2 depicts the phase diagram of the

present binary system where the nematic–isotropic (T_{NI}) and smectic-A–nematic (T_{SN}) transition temperatures of the mixtures have been plotted against the mole fractions of the hockey stick-shaped compound (compound **5**). Both the transition temperatures have been ascertained during cooling cycles with the aid of polarizing optical microscopy and the optical transmission techniques. This work is particularly focused on the region where the concentration of the guest compound is much less compared to that of the host.

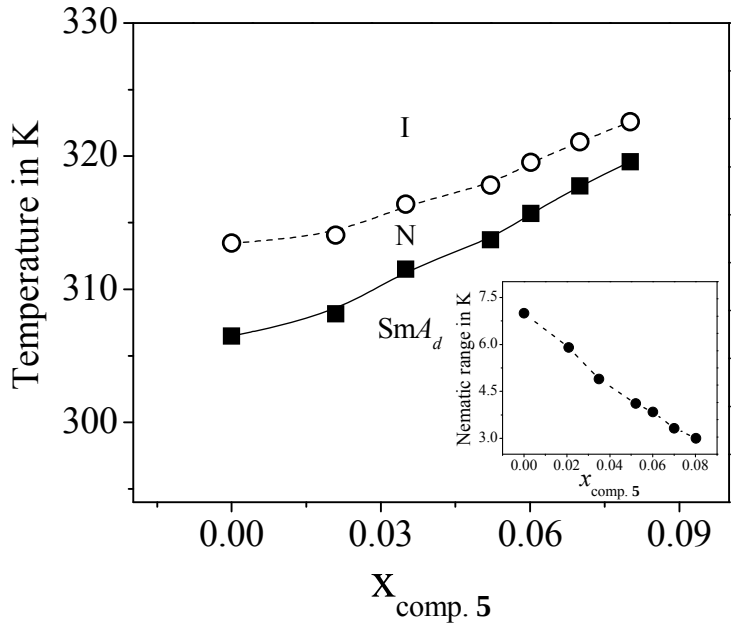

Figure 8.2. Partial phase diagram of the binary system comprising compound **5** and 8CB. $x_{\text{comp.}\mathbf{5}}$ denotes the mole fraction of compound **5**. I: isotropic phase; N: nematic phase; Sm-A_d : smectic A_d phase. ○: nematic to isotropic transition temperature; ■: smectic-A_d to nematic transition temperature. Inset shows concentration dependence of the nematic range for the present system. Dashed and solid lines are drawn for guidance to eye.

It has been observed that addition of the hockey stick-shaped molecules enhances both the *N–I* and Sm-*A–N* transition temperatures. However, the enhancement in transition temperature relating to the concentration variation is a little more gradual for the *N–I* phase transition than for the Sm-*A–N* phase transition. The variation of the nematic range against molar concentration has also been presented in the inset of figure 8.2. Nematic range has been found to

decrease from a value of 6 °C to 3 °C, where the shrinkage follows a nearly linear trend with the variation of molar concentration. It is obvious that addition of the angular mesogenic molecules leads to a destabilization of the nematic phase in the host medium and thereby decreases the nematic range.

8.4. Optical birefringence measurements

Figure 8.3 portrays an overview of the experimentally measured birefringence ($\Delta n = n_e - n_o$) values for pure 8CB at a wavelength of λ= 632.8 nm over a temperature range embracing both the nematic and smectic-*A* mesophases. Now in the present context, along with quality, the reproducibility

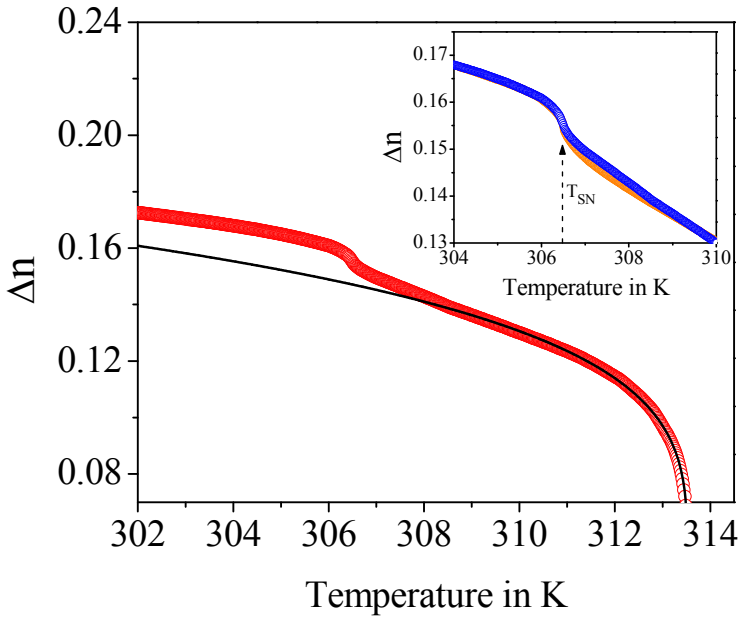

Figure 8.3. Experimental values of birefringence ($\Delta n = n_e - n_o$) for 8CB as a function of temperature. The solid line presents a fit to equation (8.3), extrapolated to the Sm-*A* phase. Inset shows comparison of the temperature dependence of birefringence close to the Sm-*A*–*N* phase transition for the same compound. ○: first run; ○: second run. Dashed vertical arrow denotes the Sm-*A*–*N* phase transition temperature (T_{SN}).

of the experimental data is also very important for extracting a proper knowledge of critical anomaly near a transition. Hence, testing of the

reproducibility of the measured Δ*n* values, particularly near the critical region, is also quite necessary. Measurements have been carried out in repeated heating and cooling cycles and the outcomes have been compared. The measured values of birefringence in two such consecutive runs are illustrated in the inset of figure 8.3. Excellent agreement has been obtained between the two sets of data with a maximum deviation of ~1%, thus certainly validating the high accuracy and reproducibility of the data from this experimental method.

The temperature dependence of the birefringence (Δ*n*) for two representative mixtures with molar concentrations $x_{\text{comp.5}}$ = 0.021 and 0.035 has also been displayed in figures 8.4(a) and 8.4(b). On cooling from the isotropic phase, a sharp enhancement in Δ*n* is observed following the *N*–*I* phase transition, essentially due to an enhancement in the nematic order. On further cooling, well within the mesophase, Δ*n* retains an identical trend but now the increase is comparatively sluggish. The resultant temperature dependence of birefringence (Δ*n*) as well as its magnitude in the mesophase is fairly in accord with those reported by others employing refractometers [43] and a high resolution rotating-analyzer technique [44]. However, the resolution of the present data is comparatively higher relative to the refractometer data but comparable with those obtained from the rotating-analyzer method. From figures 8.3 and 8.4 it is apparent that all the Δ*n* *vs.* *T* curves are accompanied with a small but finite measurable change in birefringence (Δ*n*) on entering the Sm-*A* phase, essentially due to the impartation of translational ordering into the mesophase structure. Moreover, there is no noticeable discontinuity in the Δ*n* curves at the Sm-*A*–*N* phase transition. This birefringence measurement has been succeed in probing the transitional variation quite accurately, thus facilitating a more insightful description of that transition.

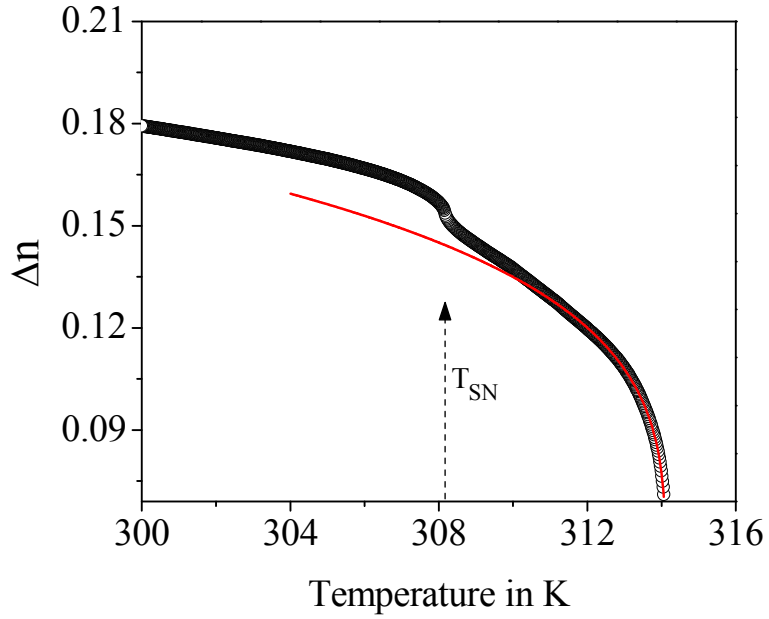

(a)

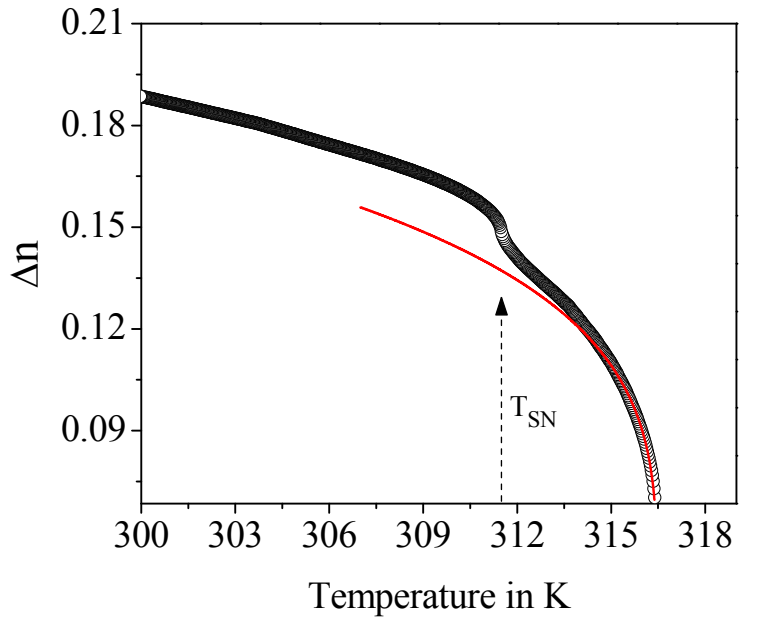

(b)

Figure 8.4. Experimental values of birefringence ($\Delta n = n_e - n_o$) as a function of temperature for different mixtures. (a) $x_{comp.5} = 0.021$, (b) $x_{comp.5} = 0.035$. Solid lines present fit to equation (8.3), extrapolated to the Sm-*A* phase. Dashed vertical arrow denotes the Sm-*A*–*N* phase transition temperature (T_{SN}).

8.5. Critical behavior at the *N–I* phase transition

According to theoretical requirements, a faithful manifestation of the optical characteristics of a liquid crystalline media needs a precise reckoning of the local field surrounding a molecule. Now, in order to probe the exact behavior of the scalar order parameter $S(T)$ [35], specifying the orientational ordering of a nematic mesogenic medium, one necessitates a theoretical model relating particular macroscopic and microscopic properties of the concerned medium. In this connection the two most widely accepted models are – (i) the isotropic internal field model, proposed by of Vuks, Chandrasekhar, and Madhusudana (VCM model) [45, 46], and (ii) the anisotropic internal field model of Neugebauer, Maier, and Saupe (NMS model) [47–49]. Under the conjecture of the isotropic nature of the local molecular field (i.e., VCM model), one may relate molecular polarizability (α) of a mesogenic medium with the birefringence (Δn) of the same through the following relation:

$$\frac{\Delta\alpha}{\langle\alpha\rangle}S(T) = \frac{\Delta(n^2)}{\langle n^2\rangle - 1} \tag{8.1}$$

where $\Delta(n^2) = n_e^2 - n_o^2$ is the anisotropy of the square of the refractive index; $\langle n^2\rangle = (n_e^2 + 2n_o^2)/3$ and n_e and n_o are, respectively, the extraordinary and ordinary components of the refractive index. The molecular polarizability anisotropy is termed as $\Delta\alpha = \alpha_l - \alpha_t$ and the mean polarizability $\langle\alpha\rangle = (\alpha_l + \alpha_t)/3$ where α_l and α_t are the longitudinal and transverse polarizibilities with reference to the long molecular axis, respectively.

Moreover, in an attempt to precisely probe the temperature dependence of the nematic order parameter, one may take the recourse of a four-parameter power-law expression, which is in accord with the mean-field theory for both critical and tricritical behaviors of weakly first-order transitions [38, 50],

$$S(T) = S^{**} + A\left|\left(1 - \frac{T}{T^*}\right)\right|^{\beta} \tag{8.2}$$

where, T^{**} is the temperature corresponding to the effective second-order transition point, i.e., the absolute limit of superheating of the nematic phase and slightly higher than the observed *N–I* transition temperature (T_{NI}); at $T = T^{**}$, $S(T^{**}) = S^{**}$ and β represents the critical exponent.

Equations (8.1) and (8.2) may suitably be coupled and modified with the introduction of appropriate scaling condition and few approximations yielding [43, 51, 52]

$$S(T) = \zeta \left[S^{**} + (1 - S^{**}) \left| \left(1 - \frac{T}{T^*}\right) \right|^{\beta} \right] \tag{8.3}$$

where, $\zeta = (\Delta\alpha/\alpha)[(n_I^2 - 1)/2n_I]$ and n_{I} is the refractive index in the isotropic phase just above T_{NI}. This equation contains four fit parameters, ζ, S^{**}, T^{**}, and β, and is found to be superior to the previous efforts to fit the temperature variation of Δn by means of Haller's procedure [53] which involves a relatively smaller number of fit parameters. Additionally, the Haller's method frequently yields comparatively lower values of β with $\beta \leq 0.2$ and is also quite unsuited for its incompatibility with the weakly first-order character of the *N–I* phase transition [50].

In this study, in an attempt to characterize the critical anomaly associated with the *N–I* phase transition, the temperature dependences of Δn for pure 8CB as well as that for few other mixtures ($x_{\mathrm{comp.5}}$ = 0.0209, 0.0350, and 0.0521) are fitted with equation (8.3). Fits to the data have been displayed as solid lines in figures 8.3 and 8.4 and corresponding outcomes for the fit parameters are listed in table 8.1. The qualities of the fits have been assessed with the aid of a reduced error function χ_v^2 which is defined as the ratio of the variance of the fit (s^2) to the variance of the experimental data (σ^2) [54],

$$\chi_v^2 = \frac{s^2}{\sigma^2} = \frac{1}{N-p} \sum_i \frac{1}{\sigma_i^2} \left(\Delta n_i^{obs} - \Delta n_i^{fit} \right)^2 \tag{8.4}$$

where, N is the total number of data points, p is the number of adjustable parameters, Δn_i^{fit} is the i^{th} fit value corresponding to the measurement Δn_i^{obs}, and σ_i is the standard deviation corresponding to Δn_i^{obs}. For an ideal fit χ_v^2

value equals unity but, in general, values ranging between 1 and 1.5 yield good fits. To facilitate a consistent fitting, a few data points have been eliminated successively from either ends of the nematic range in order to get rid of the nematic–isotropic coexistence region at the high-temperature end as well as to preclude the appearance of the pretransitional effect in the vicinity of the Sm-*A*–*N* phase transition. Such a range shrinkage excludes a considerable number of data points from the fit process and for the highest concentration considered, i.e., $x_{\text{comp.5}} = 0.052$; it leaves only 1 K of usable data range, which again has clearly been signaled by the comparatively larger uncertainty associated with the corresponding β value. Such limitation also restricts the applicability of the above fit procedure for mixtures with still higher concentrations (i.e., $x_{\text{comp.5}} = 0.06$-0.08), i.e., for those with relatively smaller

Table 8.1. Values of the fit parameters obtained from the four-parameter fit of the temperature dependence of Δn to equation (8.3).

$x_{\text{comp.5}}$	ζ	S^{**}	T^{**} *in K*	β	χ_v^2
0	0.310 ± 0.005	0.13 ± 0.03	313.54 ± 0.10	0.245 ± 0.012	1.14
0.021	0.324 ± 0.004	0.11 ± 0.02	314.11 ± 0.07	0.249 ± 0.009	1.05
0.035	0.332 ± 0.009	0.09 ± 0.03	316.47 ± 0.15	0.250 ± 0.021	1.23
0.052	0.341 ± 0.014	0.08 ± 0.04	317.92 ± 0.28	0.251 ± 0.034	1.09

extent of nematic phase. As reflected from table 8.1, the extracted β values have been found to lie between 0.245 and 0.251 for the different concentrations considered and thereby are in excellent agreement with the tricritical hypothesis (TCH) ($\beta_{\text{TCH}} = 0.25$) of Keyes [36] and Anisimov *et al.* [37, 38]. Fit quality remains almost unaffected if β is kept fixed at 0.25. The outcomes for 8CB are also in line with those reported by Chirtoc *et al.* from precise refractive index measurement [43]. Moreover, an identical behavior has also been revealed for a number of nematogenic and smectogenic compounds as

well as their mixtures from diverse experimental approaches including specific heat capacity, birefringence, dielectric and volumetric measurements [52, 55–61]. Thus the present study once again confirms the validity of the tricritical nature of the *N–I* phase transition and discards the possibility of higher β values as ascertained by the critical hypothesis and also that required for describing an Ising system with nearest neighbor interactions.

8.6. Critical behavior at the Sm-*A*–*N* phase transition

The Sm-*A*–*N* phase transition in mesogenic media can always be endowed with a consequent enhancement in the orientational ordering, provoked by the mutual coupling between the nematic and smectic-*A* order parameters. It may be shown [44, 51, 52, 55, 62] that the characteristic behavior of the order parameter $S(T)$ near the Sm-*A*–*N* phase transition can be exploited to extract a quite accurate description of the critical fluctuation associated with that transition and hence to evaluate a critical exponent α' matching with the relevant specific heat capacity exponent α, which again is found to appear in an expression depicting the temperature dependence of the smectic-*A* order parameter (Ψ), as follows [63–65]

$$\langle|\Psi|^2\rangle = U \pm V^{\pm}\left|\left(\frac{T}{T_{SN}} - 1\right)\right|^{\kappa} \tag{8.5}$$

where κ = 1-α, T_{SN} corresponds to the Sm-*A*–*N* phase transition temperature, and the + and – signs refer to quantities above and below T_{SN}, respectively. Following the conjectures of the mean-field model one may stipulate the quantity (S - S_0) to be proportional to $\langle|\Psi|^2\rangle$, where S_0 is the nematic order parameter in absence of any smectic ordering [63, 66]. Moreover, to a first approximation, $S \propto \Delta n$. Hence, it is plausible to assume that the behavior of Δn at the Sm-*A*–*N* phase transition is also governed by an identical power-law divergence at a second-order phase transition as that of the specific heat capacity data with an identical critical exponent α. A similar character has also been found to be valid for the critical temperature dependence of the isobaric

thermal expansion coefficient and the isothermal compressibility coefficient, obtained from precise molar volume measurements [67, 68].

In the present investigation, despite the presence of a substantial pretransitional change, the Δn curves do not exhibit any visible discontinuity near the Sm-*A*–*N* phase transition. However, the extremum of the temperature derivative of Δn may be utilized to exactly locate the said transition. Furthermore, the quantity $n' = -d(\Delta n)/dt$ has been found to be related to the specific heat capacity anomaly [16, 52] and may be analyzed to take a proper look into the critical variance coupled with that transition. Yet, because of the small temperature interval between the two consecutive measured data, the numerically obtained first-order temperature derivative of Δn is too scattered and is not properly suited for the present analysis. Hence, it is reasonable to assume a new differential quotient having the following form [52]:

$$Q(T) = -\frac{\Delta n(T) - \Delta n(T_{SN})}{T - T_{SN}} \tag{8.6}$$

where $\Delta n(T_{SN})$ is the birefringence value at the transition temperature T_{SN}, identified by differentiating the measured Δn values. Such an incompatibility of

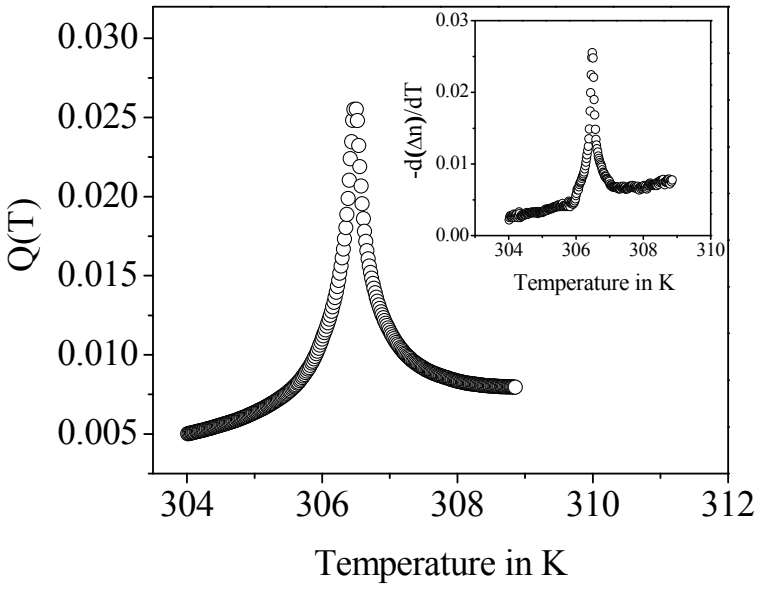

Figure 8.5. Temperature dependent variation of $Q(T)$ for pure 8CB. Inset shows temperature dependence of $-d(\Delta n)/dt$ for the same compound.

$-d(\Delta n)/dt$ is also clearly reflected from the representative temperature dependence of *Q(T)* and $-d(\Delta n)/dt$ for pure 8CB, as illustrated in figure 8.5. The quantity *Q(T)* is rather similar to the term $C(T) = -[H(T) - H(T_C)]/[T - T_C]$ appearing in the adiabatic scanning calorimetry measurement [13] with $H(T)$ being the temperature-dependent enthalpy, and similar to the correspondence between $C(T)$ and C_p [= $(dH/dT)_p$], *Q(T)* and n' also share the same power-law behavior with an identical critical exponent α' related to the transitional singularity. Previously, a similar quotient [68] was also chosen by others for studying the critical anomaly at the Sm-*A*–*N* transition from molar volume measurements as well. In this study, in an attempt to describe the limiting behavior of the quotient $Q(T)$ at the Sm-*A*–*N* phase transition, the following renormalization group expression including the corrections to scaling has been used [16, 44]:

$$Q(T) = A^{\pm}|\tau|^{-\alpha'}(1 + D^{\pm}|\tau|^{\Delta}) + E(T - T_{SN}) + B \qquad (8.7)$$

Here, $\tau = (T - T_{SN})/T_{SN}$, the superscripts ± denote those above and below T_{SN}, $A^{\pm}$ refers to the critical amplitudes, α' is the critical exponent similar to the specific heat critical exponent α, $D^{\pm}$ are the coefficients of the first corrections-to-scaling terms, Δ is the first corrections-to-scaling exponent. Theoretically, the expected value of Δ is 0.524 for a 3D-*XY* case and in this analysis it is set fixed at 0.5 without any further variation [16, 17]. *B* is a constant presenting the combined critical and regular backgrounds while the term $E(T - T_{SN})$ corresponds to a temperature-dependent part of the regular background contribution. According to theoretical considerations, the 3D-*XY* universality class demands the occurrence of a critical amplitude ratio (A^-/A^+) of 0.971, a critical exponent (α) of -0.007 and (D^-/D^+) ~ 1, while for a tricritical point the critical amplitude ratio (A^-/A^+) is nearly 1.6, critical exponent (α) is equal to 0.5, and (D^-/D^+) is close to unity.

An overview of the temperature-dependent variation of $Q(T)$ for pure 8CB as well as those for the six other mixtures comprising the hockey stick-

shaped molecules has been shown in figure 8.6. The fits to equation (8.7) are displayed as solid lines while the corresponding fit values have been listed in table 8.2. In all the fits, data very close to the transition are excluded for the presence of experimental uncertainty and sample inhomogeneity. To locate the best possible fit range, dependence of the fit parameters on the data range shrinkage has also been investigated. Fits have been carried out for different temperature limits (i.e., $|\tau|_{max}$ and $|\tau|_{min}$) and values corresponding to which the extracted parameters remain practically stable for a small change in temperature range along with a minimum regular pattern in the residuals have been selected [69].

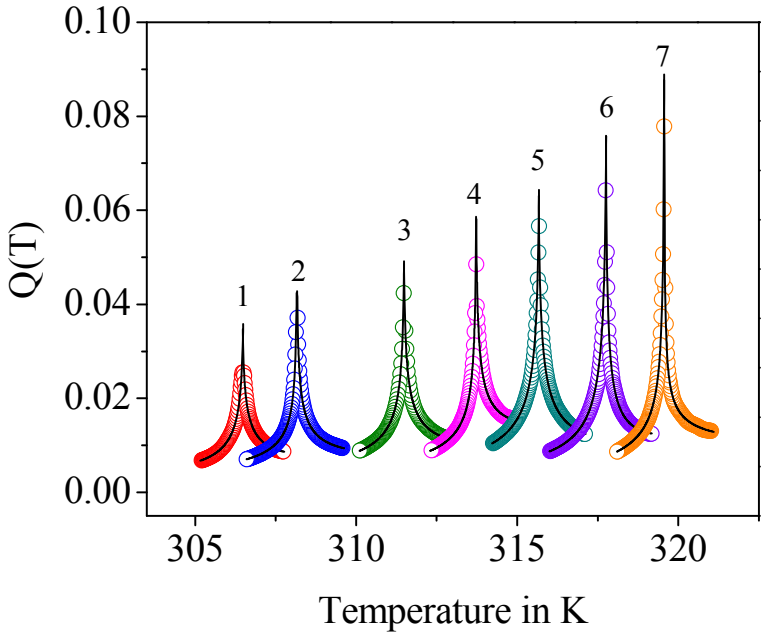

Figure 8.6. Temperature dependent variation of the quotient $Q(T)$ in the vicinity of smectic-*A*–nematic phase transition at different mole fractions x of compound **5** in the mixtures of compound **5** and 8CB. Data are arranged in sequence of increasing mole fraction x of compound **5** from left to right with 1: 8CB; 2: $x_{\text{comp.5}} = 0.021$; 3: $x_{\text{comp.5}} = 0.035$; 4: $x_{\text{comp.5}} = 0.052$; 5: $x_{\text{comp.5}} = 0.06$; 6: $x_{\text{comp.5}} = 0.07$; 7: $x_{\text{comp.5}} = 0.08$. The solid lines are fit to equation (8.7).

Table 8.2. Results corresponding to the best fit for $Q(T)$ near Sm-*A*–*N* phase transition obtained in accordance with equation (8.7) and related χ_v^2 values associated with the fits. $|\tau|_{max}$ presents the upper limit of reduced temperature considered for these fits.

$x_{\text{comp.5}}$	α'	A^-/A^+	D^-/D^+	$\lvert\tau\rvert_{max}$	χ_v^2
0	0.319 ± 0.009	1.05 ± 0.07	1.02 ± 0.05	4.4×10^{-3}	1.10
0.021	0.359 ± 0.019	0.97 ± 0.14	1.13 ± 0.16	4.4×10^{-3}	1.07
0.035	0.390 ± 0.011	1.06 ± 0.08	1.00 ± 0.19	4.3×10^{-3}	1.04
0.052	0.407± 0.010	0.88 ± 0.05	1.31 ± 0.24	4.2×10^{-3}	1.16
0.060	0.426± 0.008	1.19 ± 0.12	1.10 ± 0.12	4.4×10^{-3}	1.30
0.070	0.453± 0.017	1.28 ± 0.09	0.81 ± 0.07	4.4×10^{-3}	1.12
0.080	0.460± 0.016	1.48 ± 0.22	1.01 ± 0.08	4.3×10^{-3}	1.22

In each preliminary fit, the transition temperatures were first isolated by resolving the maxima of the temperature variation of $-d(\Delta n)/dt$ and then were kept fixed at these values. This helps in reducing the instability appearing in the least-squares minimization to a considerable extent. The goodness of the fit has been assessed with the aid of the same reduced error function χ_v^2 as defined in equation (8.4) with Δn being replaced by the corresponding $Q(T)$. The concentration dependence of the critical exponent α' for the present investigated system including that for the pure 8CB is displayed in figure 8.7 while the variation of the same against the McMillan ratio (i.e., T_{SN}/T_{NI}) has been illustrated in figure 8.8. For pure 8CB, α' comes out to be 0.319 ± 0.009 while both the quotients A^-/A^+ and D^-/D^+ assume values close to unity. These values are in excellent agreement with those obtained from high-resolution calorimetry measurements by Thoen and co-workers [13] and also those reported by Kasting *et al.* [70]. Recently, from precise Δn measurements by rotating-analyzer technique, Çetinkaya *et al.* have also proposed an α value,

quite identical to the present outcome [44]. Hence, the outcomes from the present measuring procedure once again validate the conformity between the effective critical exponents α' and α obtained from the birefringence and calorimetric measurements, respectively. For the lowest concentration considered, i.e., $x_{\text{comp.5}} = 0.021$, the exponent α' takes on a value of 0.359 ± 0.019 and then enhances monotonically with the increase in the concentration x of the angular mesogen, reaching a value of $\alpha' = 0.460 \pm 0.016$ for the highest concentration considered, i.e., $x_{\text{comp.5}} = 0.08$. Both the quotients incorporating the critical amplitudes and the corrections-to-scaling terms remain nearly unity for most of the mixtures, indicating a symmetry of the $Q(T)$ wings in the Sm-A and N phases. An examination of figures 8.7 and 8.8 reveals that an extrapolation of a quadratic fit to the extracted α' values yields a tricritical nature (i.e., where the Sm-A–N transition undergoes a crossover from second-order to first-order character) for a composition with $x_{\text{comp.5}} \sim 0.105$ with $\alpha' = 0.5$, while the corresponding McMillan ratio is 0.9936. Although the

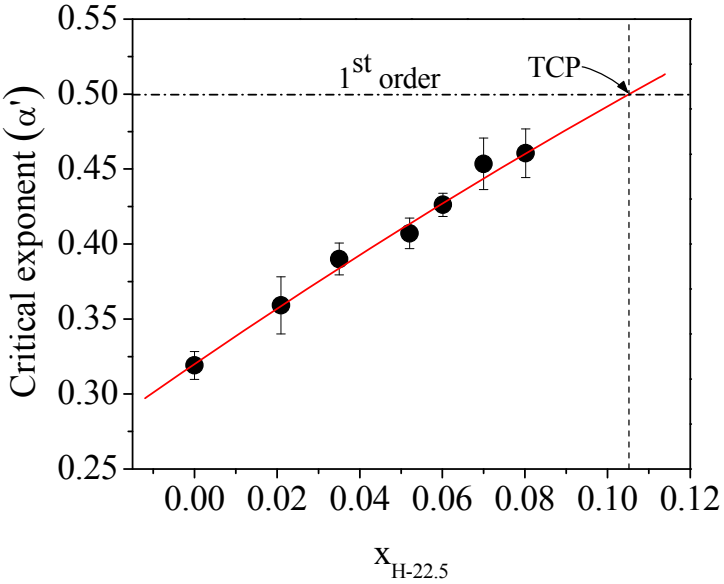

Figure 8.7. Concentration dependence of the critical exponent (α') obtained by fitting $Q(T)$ to equation (8.7). The vertical dashed line corresponds to the tricritical point (TCP). The solid line is a second-order polynomial fit to the data.

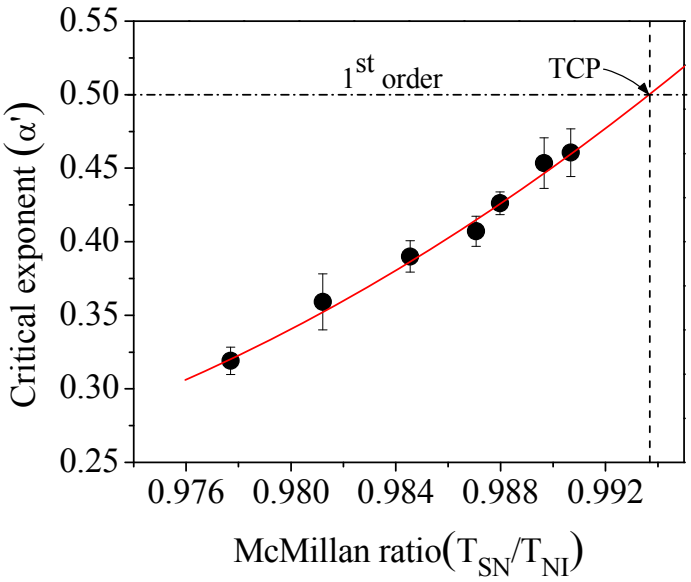

Figure 8.8. Variation of the critical exponent (α') with McMillan ratio (T_{SN} /T_{NI}). The vertical dashed line corresponds to the tricritical point (TCP). The solid line is a second-order polynomial fit to the data.

concentration variation of α' exhibits a fairly regular trend with the McMillan ratio, no such regular pattern has been observed for both A^-/A^+ and D^-/D^+ in going from one end of this system to the other.

Moreover, as stated above, $(S - S_0) \propto \langle|\Psi|^2\rangle$, where S_0 is the nematic order parameter in absence of any smectic ordering and Ψ presents the Sm-*A* order parameter [63, 66]. Hence, an attempt has also been made to analyze the critical behavior below the Sm-*A*–*N* transition using the following expression:

$$\Delta n = U\tau'^{z} + V\tau' + W \qquad (8.8)$$

where $\tau' = (1 - T/T_{SN})$ and z gives the critical coefficient. W again is the combined critical and regular background term while $V\tau'$ presents the temperature-dependent part of the regular background. The variation of Δn below the Sm-*A*–*N* transition as a function of the reduced temperature τ' for three representative mixtures with concentrations $x_{\text{comp.5}}$ = 0.02, 0.052, 0.07 is shown in figure 8.9. The fits to equation (8.8) are displayed as solid lines while the corresponding fit values are listed in table 8.3. Such a scaling to the

birefringence data leads to a z value of 0.556 ± 0.004 for $x_{\text{comp.5}} = 0.021$, which is then found to decrease with increasing hockey stick-shaped molecule concentration and reaches a value of 0.516 ± 0.01 for the highest concentration studied i.e., $x_{\text{comp.5}} = 0.08$. Moreover, from the Landau-de Gennes theory it has been envisaged that this exponent z is equal to (1-α) which again has been found to be valid for a few mesogenic systems [65]. For a number of mesogens it has been observed that $z < (1 - \alpha)$ [65]. Furthermore, for a system with true long-range order, scaling theory requires $z = 2\beta$ with β giving the critical exponent related to the limiting behavior of order parameter at the Sm-*A*–*N* phase transition. Hence, it is plausible to expect the z values to lie in a region $2\beta \leq z \leq (1 - \alpha)$. In the present study, the extracted z values are found to be relatively smaller than the computed (1-α) values with $\alpha = \alpha'$ being taken from fits to equation (8.7) and thus discard the possibility of the equality, $z = (1 - \alpha)$. Interestingly, an extrapolation to a quadratic fit to the yielded $z/2$ values defines a tricritical point at a McMillan ratio of 0.9933 (figure 8.10) which is again in excellent conformity with that yielded by the fit to α' values. Therefore, in the present case it can safely be considered that $\beta \simeq z/2 = \beta'$. As a further confirmation, the related susceptibility critical exponent γ' has also been estimated following the Rushbrooke equality [71],

$$\alpha + 2\beta + \gamma = 2 \tag{8.9}$$

with $\alpha = \alpha'$, $\beta = \beta'$, and $\gamma = \gamma'$. The variation of the γ' thus obtained has been plotted in the inset of figure 8.10. It has been observed that γ' lies within the range $1.02 \leq \gamma' \leq 1.10$ for the different mixtures, which is again in line with those expected for systems exhibiting crossover character, i.e., between γ = 1 and 1.316 expected for a tricritical and 3D-*XY* system, respectively. Hence, the estimated γ' value also definitely indicates the validity of $z \simeq 2\beta$ in the present case.

Table 8.3. Values of the fit parameters obtained from the fit of the temperature dependence of Δn to equation (8.8).

$x_{\text{comp.5}}$	U	$\beta'(=z/2)$	V	W	χ_v^2
0	0.240± 0.042	0.289± 0.006	-0.329± 0.012	0.15552± 0.00008	1.15
0.021	0.238± 0.006	0.278± 0.002	-0.244± 0.008	0.15335± 0.00003	1.09
0.035	0.246± 0.008	0.271± 0.003	-0.116± 0.02	0.14851± 0.00005	1.10
0.052	0.276± 0.010	0.271± 0.004	-0.354± 0.031	0.14704± 0.00004	1.08
0.060	0.296± 0.013	0.260± 0.004	-0.511± 0.036	0.13968± 0.00010	1.19
0.070	0.270± 0.024	0.252± 0.007	-0.649± 0.075	0.14532± 0.00017	1.27
0.080	0.234± 0.015	0.258± 0.005	-0.510± 0.040	0.15136± 0.00012	1.25

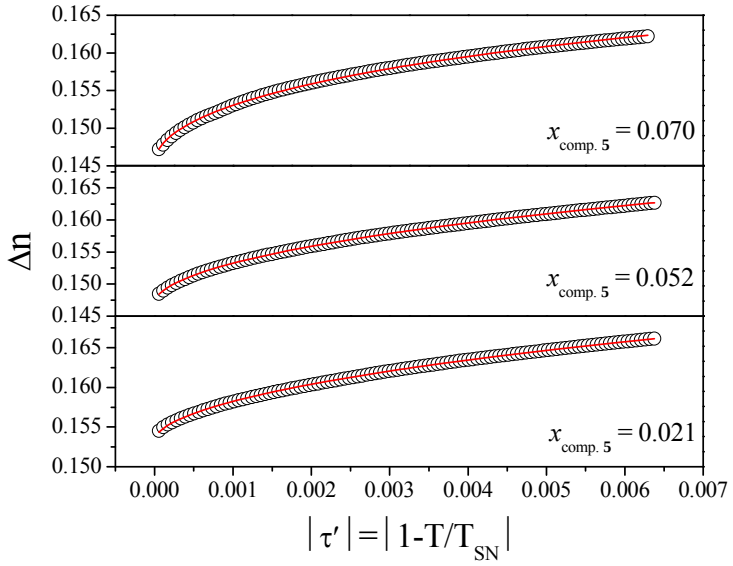

Figure 8.9. Plot of birefringence (Δn = n_e - n_o) as a function of reduced temperature $|\tau'| = |1 - T/T_{SN}|$ for different mixtures. The solid lines are fit to equation (8.8).

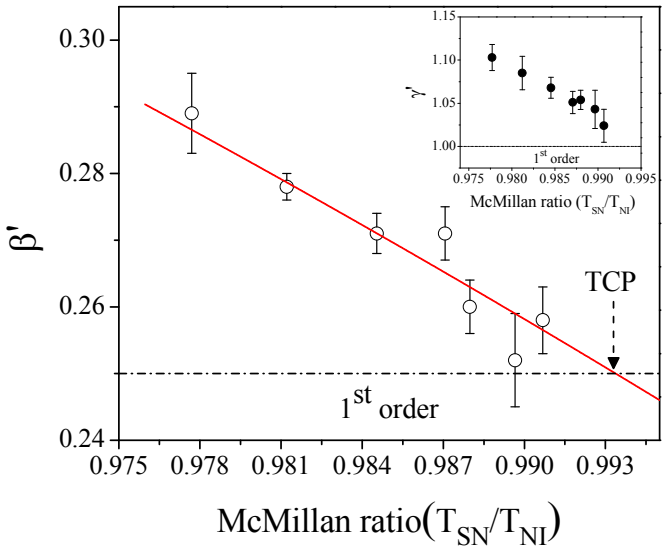

Figure 8.10. Variation of order parameter critical exponent (β') with McMillan ratio (T_{SN}/T_{NI}). The solid line is a second-order polynomial fit to the data. Inset shows variation of susceptibility critical exponent (γ') with McMillan ratio (T_{SN}/T_{NI}).

Hence, crossover behavior has been revealed by the present investigated system. The effective critical exponents (α', β', γ'), as obtained from the optical transmission measurements, assume values in between those predicted by the 3D-*XY* and tricritical hypothesis while the critical amplitude quotient corresponding to α' measurement (i.e., A^-/A^+) also offers magnitudes disagreeing with both of the above two models. It is obvious that introduction of the hockey stick-shaped molecules in the rod-like environment leads to a modification in the effective intermolecular interactions in the host medium. Enhancement of concentration of the dopant compound causes an augmentation of such resultant effect which is again facilitated through a consequent enhancement in the associated Sm-*A*–*N* phase transition temperature. Besides, such a revision in the intermolecular interactions is also followed by a corresponding strengthening of the coupling between the nematic and smectic-*A* order parameters, thus driving the transition towards a first-order nature. McMillan ratios of 0.9936 and 0.9933 as attained by extrapolating

polynomial fits to the exponents α' and β', respectively, over the investigated concentration range, up to the tricritical composition, are in agreement with the previous reports for the Sm-*A*–*N* tricritical points. Moreover, the corrections-to-scaling quotient (i.e., D^-/D^+) related to α' also yields nonuniversal values, thus validating the inference of crossover behavior as put forward by both the exponents α' and β'.

Thus, the addition of the bent-shaped dopant has conveyed a significant impact on the phase behavior of the investigated calamitic host. The principal features relating modification in transitional behavior of the calamitic compound due to the addition of such bent-mesogenic molecules may be summarized as (i) enhancement of both the Sm-*A*–*N* and *N*–*I* phase transition temperatures with increasing dopant concentration, (ii) a narrowing of the nematic range, and (iii) consequent augmentation in the effective critical exponent α' along with a decrease in the exponents β' and γ' associated with the Sm-*A*–*N* phase transition. In an attempt to achieve a qualitative idea regarding such enhancement of transition temperatures, one may consider a comparison between the amplitude of the effective intermolecular interaction energy among the host LC molecules ($F_{\text{lc-lc}}$) and that between the host LC and dopant LC molecules ($F_{\text{lc-dp}}$). In the present case, the attractive intermolecular interaction is probably stronger for the host LC– dopant LC pair than the host LC–host LC pair, i.e., $F_{\text{lc-dp}} > F_{\text{lc-lc}}$, thus increasing local molecular ordering and elevating the transition temperatures. Moreover, the shrinkage of the nematic phase also points towards the fact that addition of the hockey stick-shaped molecules stabilizes the Sm-*A* phase. Recently, an expansion of the nematic range has been reported by Denolf *et al.* for mixtures involving pure 8CB and non-mesogenic additive biphenyl [72]. For the Sm-*A*–*N* phase transition, they have observed a decrease in the effective value of the exponent α with the increase in dopant concentration and explained this by considering a coupling term of the solute mole fraction with the nematic and smectic-*A* order parameters, appearing in the mean-field free energy density expression. Moreover, the Sm-

A–N transition temperatures appearing in Ref. [72] always display a descending trend against the enhancement of doping concentration. Such outcomes appears to be quite inevitable as for a non-mesogenic impurity one may expect $F_{\text{lc-dp}} < F_{\text{lc-lc}}$, which again lead to a decrease in the associated local molecular ordering along with a fall in the related transition temperature. A decrease in transition temperature has also been revealed for other nonmesogenic additives [73] and confinement in aligned aerosil gels as well [74]. However, to the contrary, Sasaki *et al.* have recently found that for systems comprising the *n*-alkyloxy-cyanobiphenyl and a bent-core dopant, the nematic–smectic-A_d transition temperature decreases sharply with the enhancement of the dopant concentration [11]. The effective critical exponent has been found to lie between the 3D-*XY* and tricritical value for most of the mixtures. They have observed that in their investigated case, the addition of bent-shaped dopant leads to a stabilization of the nematic phase and a corresponding destabilization of the Sm-A_d phase. Such a contradicting feature may be due to the manner of interaction undertaken by the bent-core molecules as well as their particular arrangement appearing in the calamitic background.

8.7. Conclusions

A temperature scanning measurement of optical birefringence has been undertaken to study phase behavior of a binary system consisting of the rod-like octylcyanobiphenyl (8CB) and a laterally methyl substituted hockey stick-shaped mesogen, 4-(3-*n*-decyloxy-2-methyl-phenyliminomethyl)phenyl 4-*n*-dodecyloxycinnamate (compound **5**). The precise Δn data are quite successful in characterizing the transitional anomaly associated with both the *N–I* and Sm-*A–N* phase transitions. For the investigated mixtures, the values of the critical exponent β related to the limiting behavior of the nematic order parameter close to the *N–I* phase transition, have been found to be close to 0.25 and thus are in agreement with the tricritical hypothesis; this also excludes the possibility of any higher β values.

Emphasis has also been given to temperature dependence of the birefringence close to the Sm-*A*–*N* phase transition along the path of concentration variation. No visible discontinuity was observed at the Sm-*A*–*N* phase transition implying a second-order nature of that transition. Power-law analysis of the data successfully describes the divergence of the differential quotient $Q(T)$ extracted from Δn on both sides of the transition over a broad range of reduced temperature. It has been observed that the introduction of the angular mesogenic dopant leads to a contraction of the nematic range with a corresponding enhancement in the $Q(T)$ anomaly near the Sm-*A*–*N* phase transition. The yielded effective critical exponent (α') values were found to be non-universal in nature, i.e., being intermediate between those predicted for 3D-*XY* and tricritical systems. For the pure 8CB, the evaluated α' value has been found to be in excellent agreement with those obtained from the high-resolution adiabatic scanning calorimetry and birefringence measurements by others. Moreover, the exponents β' and γ' as extracted from fits to the Δn data, were also found to support the crossover character as put forwarded by the α' variation. One conspicuous aspect of the present investigated system is the considerable influence of the curved mesogenic entities on the resultant de Gennes $S - |\Psi|$ coupling between the nematic and smectic-*A* order parameter in the host medium. Undoubtedly the intermolecular interactions get revised on a significant scale by the presence of the bent molecules in the "sea" of the rodlike hosts, thus affecting the order of the transition, where perhaps the kinked molecular shape of the dopant also plays an important role. However, manifestation of the exact dependence of the order character of the Sm-*A*–*N* phase transition on the molecular profile and also exact treatment of the interactions on a molecular level relating the transitional anomaly decided by the various coupling forces, is beyond the scope of the present work and necessitates future seminal works incorporating both theoretical and experimental approaches for distinct dopant-host pairs with diverse core structures and molecular profiles. Hence, systems involving nonlinear

mesogenic impurity are likely to emerge as a viable route providing rich insight into the unexplored aspects of transitional fluctuations and henceforth lead to a better understanding of the physics of phase transition and critical phenomena in soft matter systems.

References:

[1] J. Thisayukta, H. Niwano, H. Takezoe, and J. Watanabe, *J. Am. Chem. Soc.*, **124**, 3354 (2002).

[2] M. Nakata, Y. Takanishi, J. Watanabe, and H. Takezoe, *Phys. Rev. E*, **68**, 041710 (2003).

[3] E. Gorecka, M. Čepič, J. Mieckowski, M. Nakata, H. Takezoe, and B. Žekš, *Phys. Rev. E*, **67**, 061704 (2003).

[4] R. Prathibha, N. V. Madhusudana, and B. K. Sadashiva, *Science*, **288**, 2184 (2000).

[5] R. E. Gorecka, M. Nakata, J. Mieczkowski, Y. Takanashi, K. Ishikawa, J. Watanabe, H. Takezoe, S. H. Eichhorn, and T. M. Swager, *Phys. Rev. Lett.*, **85**, 2526 (2000).

[6] K. Kishikawa, N. Muramatsu, S. Kohmoto, K. Yamaguchi, and M. Yamamoto, *Chem. Mater.*, **15**, 3443 (2003).

[7] B. Kundu, R. Pratibha, and N. V. Madhusudana, *Phys. Rev. Lett.*, **99**, 247802 (2007).

[8] T. Otani, F. Araoka, K. Ishikawa, and H. Takezoe, *J. Am. Chem. Soc.*, **131**, 12368 (2009).

[9] C. Zhu, D. Chen, Y. Shen, C. D. Jones, M. A. Glaser, J. E. Maclennan, and N. A. Clark, *Phys. Rev. E*, **81**, 011704 (2010).

[10] Y. Sasaki, K. Ema, K. V. Le, H. Takezoe, S. Dhara, and B. K. Sadashiva, *Phys. Rev. E*, **82**, 011709 (2010).

[11] Y. Sasaki, K. Ema, K. V. Le, H. Takezoe, S. Dhara, and B. K. Sadashiva, *Phys. Rev. E*, **83**, 061701 (2011).

[12] G. B. Kasting, K. J. Lushington, and C.W. Garland, *Phys. Rev. B*, **22**, 321 (1980).

[13] J. Thoen, H. Marynissen, and W. Van Dael, *Phys. Rev. A*, **26**, 2886 (1982).

[14] P. G. de Gennes and J. Prost, *The Physics of Liquid Crystals*, Oxford University Press, Oxford (1993).

[15] J. Thoen, *Physical Properties of Liquid Crystals*, D. Demus, J. Goodby, G. W. Gray, H. -W. Spiess, and V. Vill (Eds.), Wiley-VCH, Weinheim (1999).

[16] C. W. Garland, *Liquid Crystals: Experimental Study of Physical Properties and Phase Transitions*, S. Kumar (Ed.), Cambridge University Press, Cambridge (2001).

[17] C. W. Garland and G. Nounesis, *Phys. Rev. E*, **49**, 2964 (1994).

[18] K. K. Kobayashi, *Phys. Lett. A*, **31**, 125 (1970); *J. Phys. Soc. Jpn.*, **29**, 101 (1970).

[19] W. L. McMillan, *Phys. Rev. A*, **4**, 1238 (1971).

[20] J. Thoen, *Int. J. Mod. Phys. B*, **9**, 2157 (1995).

[21] B. I. Halperin, T. C. Lubensky, and S. -K. Ma, *Phys. Rev. Lett.*, **32**, 292 (1974).

[22] C. Dasgupta and B. I. Halperin, *Phys. Rev. Lett.*, **47**, 1556 (1981).

[23] M. A. Anisimov, P. E. Cladis, E. E. Gorodetskii, D. A. Huse, V. E. Podneks, V. G. Taratuta, W. van Saarloos, and V. P. Voronov, *Phys. Rev. A*, **41**, 6749 (1990).

[24] C. W. Garland, G. Nounesis, and K. J. Stine, *Phys. Rev. A*, **39**, 4919 (1989).

[25] C. W. Garland, G. Nounesis, K. J. Stine, and G. Heppke, *J. Phys.* (*Paris*), **50**, 2291 (1989).

[26] P. Das, G. Nounesis, C. W. Garland, G. Sigaud, and N. H. Tinh, *Liq. Cryst.*, **7**, 883 (1990).

[27] G. Nounesis, C. W. Garland, and R. Shashidhar, *Phys. Rev. A*, **43**, 1849 (1991).

[28] T. C. Lubensky and J. H. Chen, *Phys. Rev. B*, **17**, 366 (1978).

[29] T. C. Lubensky, *J. Chim. Phys. Phys.-Chim. Biol.*, **80**, 31 (1983).

[30] T. C. Lubensky and A. J. McKane, *Phys. Rev. A*, **29**, 317 (1984).

[31] D. R. Nelson and J. Toner, *Phys. Rev. B*, **24**, 363 (1981).

[32] J. Toner, *Phys. Rev. B*, **26**, 462 (1982).

[33] B. R. Patton and B. S. Andereck, *Phys. Rev. Lett.*, **69**, 1556 (1992).

[34] B. S. Andereck and B. R. Patton, *Phys. Rev. E*, **49**, 1393 (1994).

[35] W. Maier and A. Saupe, *Z. Naturforsch. A*, **13a**, 564 (1958); **14a**, 882 (1959).

[36] P. H. Keyes, *Phys. Lett. A*, **67**, 132 (1978).

[37] M. A. Anisimov, S. R. Garber, V. S. Esipov, V. M. Mamnitskii, G. I. Ovodov, L. A. Smolenko, and E. L. Sorkin, *Sov. Phys. JETP*, **45**, 1042 (1977).

[38] M. A. Anisimov, *Mol. Cryst. Liq. Cryst. Inc. Nonlinear Opt.*, **162**, 1 (1988).

[39] A. Chakraborty, S. Chakraborty, and M. K. Das, *Phys. Rev. E*, **91,** 032503 (2015).

[40] A. J. Leadbetter, R. M. Richardson, and C. N. Colling, *J. Phys.* (*Paris*), **36**, C1-37 (1975).

[41] J. E. Lydon and C. J. Coakley, *J. Phys.* (*Paris*), **36**, C1-45 (1975).

[42] A. Chakraborty, B. Das, M. K. Das, S. Findeisen-Tandel, M.-G. Tamba, U. Baumeister, H. Kresse, and W. Weissflog, *Liq. Cryst.*, **38**, 1085 (2011).

[43] I. Chirtoc, M. Chirtoc, C. Glorieux, and J. Thoen*, Liq. Cryst.*, **31,** 229 (2004).

[44] M. C. Çetinkaya, S. Yildiz, H. Özbek, P. Losada-Pérez, J. Leys, and J. Thoen, *Phys. Rev. E*, **88**, 042502 (2013).

[45] M. F. Vuks, *Opt. Spectrosc.*, **20**, 361 (1966).

[46] S. Chandrasekhar and N. V. Madhusudana, *J. Phys.* (*Paris*), **30**, C4-24 (1969).

[47] H. E. J. Neugebauer, *Can. J. Phys.*, **32**, 1 (1954).

[48] A. Saupe and W. Maier, *Z. Naturforsch. A*, **16a**, 816 (1961).

[49] H. S. Subramhanyam and D. Krishnamurthi, *Mol. Cryst. Liq. Cryst.*, **22**, 239 (1973).

[50] J. Thoen and G. Menu, *Mol. Cryst. Liq. Cryst.*, **97**, 163 (1983).

[51] S. Yildiz, H. Özbek, C. Glorieux, and J. Thoen, *Liq. Cryst.*, **34,** 611 (2007).

[52] S. Erkan, M. Çetinkaya, S. Yildiz, and H. Özbek, *Phys. Rev. E*, **86**, 041705 (2012).

[53] I. Haller, *Progr. Solid State Chem.*, **10**, 103 (1975).

[54] P. R. Bevington and D. K. Robinson, *Data Reduction and Error Analysis for the Physical Sciences*, McGraw-Hill, New York (2003).

[55] S. K. Sarkar, P. C. Barman, and M. K. Das, *Physica B*, **446**, 80 (2014).

[56] P. Cusmin, M. R. de la Fuente, J. Salud, M. A. Pérez-Jubindo, S. Diez-Berart, and D. O. López, *J. Phys. Chem. B*, **111**, 8974 (2007).

[57] J. Salud, P. Cusmin, M. R. de la Fuente, M. A. Pérez-Jubindo, D. O. López, and S. Diez-Berart, *J. Phys. Chem. B*, **113**, 15967 (2009).

[58] A. Drozd-Rzoska, S. J. Rzoska, and J. Zioło, *Phys. Rev. E*, **54**, 6452 (1996).

[59] S. J. Rzoska, J. Ziolo, W. Sulkowski, J. Jadżyn, and G. Czechowski, *Phys. Rev. E*, **64**, 052701 (2001).

[60] A. Prasad and M. K. Das, *Phys. Scr.*, **84**, 015603 (2011).

[61] A. Żywociński, *J. Phys. Chem. B*, **107**, 9491 (2003).

[62] S. K. Sarkar and M. K. Das, *RSC Adv.*, **4**, 19861 (2014).

[63] P. G. de Gennes, *Mol. Cryst. Liq. Cryst.*, **21**, 49 (1973).

[64] M. E. Fisher and A. Aharony, *Phys. Rev. Lett.*, **31**, 1238 (1973).

[65] K. K. Chan, M. Deutsch, B. M. Ocko, P. S. Pershan, and L. B. Sorensen, *Phys. Rev. Lett.*, **54**, 920 (1985).

[66] K. -C. Lim and J. T. Ho, *Phys. Rev. Lett.*, **40**, 944 (1978).

[67] A. Żywociński, S. A. Wieczorek, and J. Stecki, *Phys. Rev. A*, **36**, 1901 (1987).

[68] A. Żywociński and S. A. Wieczorek, *J. Phys. Chem. B*, **101**, 6970 (1997).

[69] J. A. Potton and P. C. Lanchester, *Phase Transitions*, **6**, 43 (1985).

[70] G. B. Kasting, C. W. Garland, and K. J. Lushington, *J. Phys.* (*Paris*), **41**, 879 (1980).

[71] H. E. Stanley, *Introduction to Phase Transitions and Critical Phenomena*, Clarendon Press, Oxford (1971).

[72] K. Denolf, B. V. Roie, C. Glorieux, and J. Thoen, *Phys. Rev. Lett.*, **97**, 107801 (2006).

[73] K. P. Sigdel and G. S. Iannacchione, *Phys. Rev. E*, **82**, 051702 (2010).

[74] F. Cruceanu, D. Liang, R. L. Leheny, C. W. Garland, and G. S. Iannacchione, *Phys. Rev. E*, **79**, 011710 (2009).